Analysis of Microstrip Antennas with Perturbation Segments

Takafumi FUJIMOTO, Kazumasa TANAKA, and Mitsuo TAGUCHI
Department of Electrical and Electronic Engineering,
Faculty of Engineering, Nagasaki University
1-14 Bunkyo-machi, Nagasaki-shi, 852-8521, Japan
E-mail : takafumi@net.nagasaki-u.ac.jp

1. Introduction

A number of analytical methods on microstrip antenna (MSA) have been developed. Among them, the cavity model [1] and the integral equation method [2] are often used. Although the cavity model cannot calculate an arbitrarily shaped MSA, the cavity model has the advantages of being simpler than the integral equation method and providing physical insight. In the cavity model, the wall admittance at the side apertures has to be determined in advance and its accuracy influences input impedance and resonant frequency. The wall admittances have been investigated for MSA with a patch of simple configuration [3]–[5].

The authors have proposed a formulation method for the wall admittance of an arbitrarily shaped MSA and calculated the circular MSA [6], and the elliptical MSA with and without a circular slot [7]. In [7], the cavity model applicable to the MSA with a patch whose geometry deviates from a particular coordinate system has been also proposed. The wall admittance in [6], [7] is defined by the magnetic field produced by the equivalent magnetic current on the aperture. The magnetic field is derived using Green's functions obtained by the spectral domain analysis so as to consider the dielectric substrate. The calculated input impedances and axial ratio in [6], [7] agree fairly well with the experimental data.

In this paper, the proposed method is extended to the MSAs whose patch has the corners, where the wall susceptance has the singularity. The circular and rectangular MSAs with the perturbation segments, commonly used as a single-feed circularly polarized MSA, are analyzed.

2. Theory

2.1 Circular MSA with perturbation segments

Figure 1 shows the geometry and coordinate system of the circular MSA with perturbation segments. The relative dielectric constant and thickness of the substrate are ε_r and h, respectively. The antenna is excited at r=d_0, ϕ=ϕ_0 by a coaxial feeder through the dielectric substrate. The electromagnetic fields within and outside the cavity are denoted by $\mathbf{E}^d$, $\mathbf{H}^d$ and $\mathbf{E}^e$, $\mathbf{H}^e$, respectively.

The thickness of the substrate is assumed to be much smaller than the wavelength, so the electromagnetic fields within the cavity do not vary along the z direction. Applying the continuity conditions of the electromagnetic fields between the regions 1 and 2, the electric field within the cavity $\mathbf{E}^d$ is expressed in terms of the eigenfunctions in the cylindrical coordinate system (r, ϕ, z) as,

In Region 1 $(0 \le r \le d_0)$

$$\mathbf{E}^d = \sum_{n=0}^{N} (E_{zn}^{cJ} + E_{zn}^{sJ})\mathbf{i}_z \tag{1}$$

$$E_{zn}^{cJ} = \left\{ A_n + \frac{jI_0\omega\mu_0}{2(1+\delta_n)} N_n(k_1 d_0)\cos(n\phi_0) \right\} \times J_n(k_1 r)\cos(n\phi) \tag{2}$$

$$E_{zn}^{cN} = \left\{ B_n + \frac{jI_0\omega\mu_0}{2(1+\delta_n)} N_n(k_1 d_0)\sin(n\phi_0) \right\} \times J_n(k_1 r)\sin(n\phi) \tag{3}$$

In Region 2 $(d_0 \le r \le a_0)$

$$\mathbf{E}^d = \sum_{n=0}^{N} (E_{zn}^{cJ} + E_{zn}^{sJ} + E_{zn}^{cN} + E_{zn}^{sN})\mathbf{i}_z \tag{4}$$

$$E_{zn}^{cJ} = C_n J_n(k_1 r)\cos(n\phi) \tag{5}$$

$$E_{zn}^{cN} = \frac{jI_0\omega\mu_0}{2(1+\delta_n)} J_n(k_1 d_0)\cos(n\phi_0) \times N_n(k_1 r)\cos(n\phi) \tag{6}$$

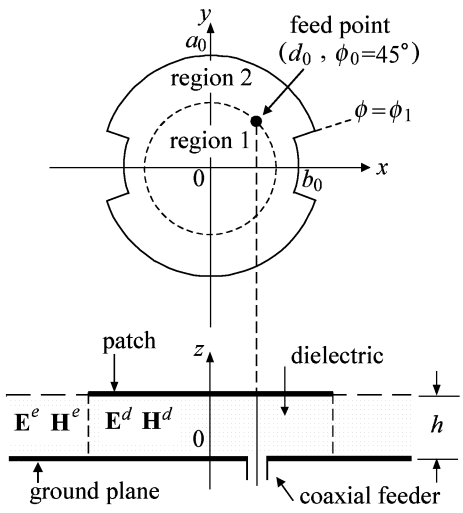

Figure 1: Geometry of circular MSA with perturbation segments

$$E_{zn}^{sJ} = D_n J_n(k_1 r)\sin(n\phi) \tag{7}$$

$$E_{zn}^{sN} = \frac{jI_0\omega\mu_0}{2(1+\delta_n)} J_n(k_1 d_0)\sin(n\phi_0) \times N_n(k_1 r)\sin(n\phi), \tag{8}$$

where $k_1 = \omega\sqrt{\mu_0\varepsilon_1} = \omega\sqrt{\mu_0\varepsilon_r\varepsilon_0}$. δ_n is zero for $n > 0$ and is equal to 1 for $n = 0$. $J_n(k_1 r)$ and $N_n(k_1 r)$ are Bessel and Neumann functions of order n, respectively. I_0 is the total current at the feed point. $\{A_n\}$ – $\{D_n\}$ are unknown coefficients.

The unknown coefficients are determined from the impedance boundary condition at the aperture;

$$\sum_{n=0}^{N}(y_n^{cJ}E_{zn}^{cJ} + y_n^{cN}E_{zn}^{cN} + y_n^{sJ}E_{zn}^{sJ} + y_n^{sN}E_{zn}^{sN}) + H_t^d = 0. \tag{9}$$

t expresses the tangential component along the aperture. The magnetic field within the cavity $\mathbf{H}^d$ is obtained by Eqs.(1)–(8) and Maxwell's equations. y_n^{cJ}, y_n^{cN}, y_n^{sJ} and y_n^{sN} are the wall admittances of order n at the aperture and are defined by the magnetic fields produced by the equivalent magnetic currents at the aperture. The magnetic fields are derived using Green's functions obtained by the spectral domain analysis [6], [7]. The superscripts cJ, cN, sJ and sN in y_n mean the wall admittances corresponding to the electric fields E_{zn}^{cJ}, E_{zn}^{cN}, E_{zn}^{sJ} and E_{zn}^{sN}, respectively.

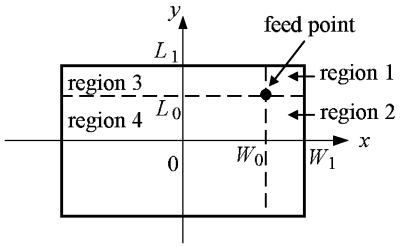

Figure 2: Geometry of rectangular MSA with perturbation segments

2.2 Rectangular MSA with perturbation segments

Figure 2 shows the geometry and coordinate system of the rectangular MSA with perturbation segments. The antenna is fed at x=W_0, y=L_0 by a coaxial feeder through the dielectric substrate.

In this paper, TM_{10} and TM_{01} modes, the primary modes of the rectangular MSA, are analyzed. In order to account for fringe fields, the effective length of the patch is assumed as $W_1+\delta_x$, $L_1+\delta_y$, where δ_x and δ_y are the edge extension.

Applying the boundary conditions between regions 1, 2, 3 and 4, the electric fields within the cavity are summarized as the following equations.

$$\mathbf{E}^d = (E_{z01}^a + E_{z01}^b + E_{z10}^a + E_{z10}^b)\mathbf{i}_z \tag{10}$$

$$E_{z01}^a = A_{01}\sin(k_{y1}y) \tag{11}$$

$$E_{z01}^b = \begin{cases} \frac{-jI_0\omega\mu_0}{8(W_1+\delta_x)k_{y1}}\sin(k_{y1}L_0)\cos(k_{y1}y) \\ \quad : \text{in Regions 1 and 3} \\ \frac{-jI_0\omega\mu_0}{8(W_1+\delta_x)k_{y1}}\cos(k_{y1}L_0)\sin(k_{y1}y) \\ \quad : \text{in Regions 2 and 4} \end{cases} \tag{12}$$

$$E_{z10}^a = A_{10}\sin(k_{x1}x) \tag{13}$$

$$E_{z10}^b = \begin{cases} \frac{jI_0\omega\mu_0}{8(L_1+\delta_y)k_{x1}}\sin(k_{x1}W_0)\cos(k_{x1}x) \\ \quad : \text{in Regions 1 and 2} \\ \frac{jI_0\omega\mu_0}{8(L_1+\delta_y)k_{x1}}\cos(k_{x1}W_0)\sin(k_{x1}x) \\ \quad : \text{in Regions 3 and 4.} \end{cases} \tag{14}$$

A_{01} and A_{10} are the unknown coefficients. k_{x1} and k_{y1} are expressed as

$$k_{x1} = \frac{\pi}{2(W_1+\delta_x)} \quad , \quad k_{y1} = \frac{\pi}{2(L_1+\delta_y)}. \tag{15}$$

On the other hand, k_{x1} and k_{y1} satisfy the following equation.

$$k_{x1} = k_{y1} = k_1 \tag{16}$$

Substituting Eq.(16) into Eqs.(15), δ_x and δ_y are determined.

The unknown coefficients A_{01} and A_{10} are determined from the impedance boundary conditions at

the aperture;

$$y^a_{01}E^a_{z01} + y^b_{01}E^b_{z01} + H^d_{t01} = 0 : \mathrm{TM}_{01} \text{ mode} \quad (17)$$
$$y^a_{10}E^a_{z10} + y^b_{10}E^b_{z10} + H^d_{t10} = 0 : \mathrm{TM}_{10} \text{ mode.} \quad (18)$$

y^a_{mn} and y^b_{mn} are the wall admittances of the TM_{mn} mode at the aperture, respectively. The superscripts a and b in y_{mn} mean the wall admittances corresponding to the electric fields E^a_{zmn} and E^b_{zmn}, respectively.

3. Results and Discussion

Figures 3 show the wall admittances $g^{cJ}_1 + jb^{cJ}_1$ and $g^{sJ}_1 + jb^{sJ}_1$ of the first mode on the circular MSA with perturbation segments. Although the wall conductances are constant along the circumference, the wall susceptances have the singularity at the corner of the perturbation segment $\phi = \phi_1$ due to the discontinuity of the derivative of the equivalent magnetic current at the corner. As in Fig. 4, the configuration of the antenna patch is approximated by the continuously smooth one that the derivative of the equivalent magnetic current on the aperture varies continuously. In Fig. 3(b), the approximate wall susceptances b^{sJ}_1 is shown. The singularity of the wall susceptance at corner of the patch vanishes.

Figure 5 shows the calculated and measured input impedances of the circular MSA with the perturbation segments. The relative error of the measured resonant frequency to the calculated one is 3.6%. The calculated minimum axial ratio is 0.84dB at 6.51GHz and the measured value is 0.71dB at 6.30GHz.

Figures 6 show the wall admittances $g^a_{10} + jb^a_{10}$ and $g^a_{01} + jb^a_{01}$ on the rectangular MSA with the perturbation segments. In both TM_{10} and TM_{01} modes, the differences of the wall conductances between the radiating aperture and the non radiating aperture are observed. The wall susceptances of the rectangular MSA with the perturbation segments have also the small singularity at the corners due to the discontinuity of the derivative of the equivalent magnetic current at the corners.

Figure 7 shows the calculated and measured input impedances of the rectangular MSA with the perturbation segments. The calculated resonant frequency and minimum axial ratio agree well with the measured ones

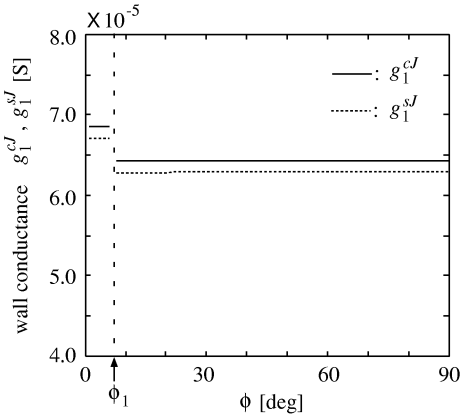

(a) Wall conductances

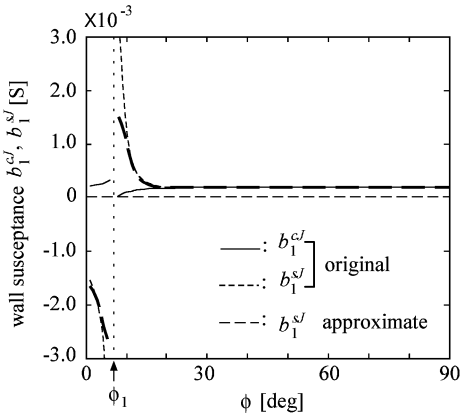

(b) Wall susceptances

Figure 3: Wall admittances of first mode of circular MSA with perturbation segments (a_0=9.0mm, b_0=8.21mm, ϕ_1=7°, h=0.764mm, ε_r=2.15, frequency=6.5GHz)

4. Conclusion

The wall admittance of the circular and rectangular MSA with perturbation segments are calculated. The wall admittance is defined by the magnetic field produced by the equivalent magnetic current at the aperture. The magnetic field has been derived using Green's functions obtained by the spectral domain analysis.

The input impedance and axial ratio calculated by the cavity model with this wall admittance agree well with the measured data. The proposed method is valid for the MSAs whose patch has the corners.

Acknowledgment

The authors would like to thank Research Associate E. Nishiyama of Saga University for his valuable advice on the measurement of MSA.

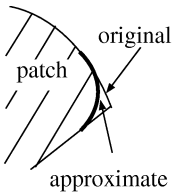

Figure 4: Approximation of antenna patch

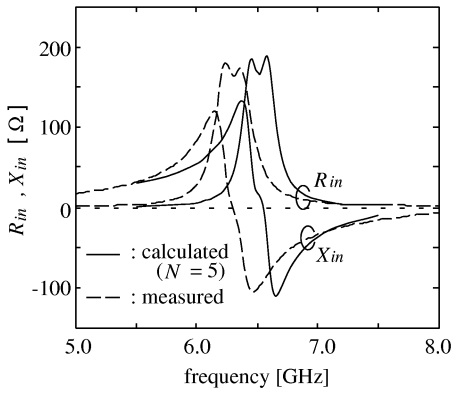

Figure 5: Input impedance of circular MSA with perturbation segments (a_0=9.02mm, b_0=8.07mm, ϕ_1=6.8°, d_0=6.0mm, h=0.764mm, ε_r=2.15, $\tan\delta$= 0.001)

References

[1] Y. T. Lo, D. Solomon and W. F. Richards, "Theory and experiment on microstrip antennas," IEEE Trans. Antennas & Propag., vol.AP-27, no.2, pp.137–145, March 1979.

[2] J. R. Mosig, "Integral equation technique," in Numerical techniques for microwave and millimeter-wave passive structures, edited by T.Itoh, pp.133–213, John Wiley & Sons, New York, 1989.

[3] A. G. Derneryd, "Linearly polarized microstrip antennas," IEEE Trans. Antennas & Propag., vol.AP-24, no.6, pp.846–851, Nov. 1976.

[4] L. C. Shen, "Analysis of circular-disc printed-circuit antenna," Proc. IEE, vol.126, no.12, pp.1220–1222, Dec. 1979.

[5] A. K. Bhattacharyya and R. Garg, "Input impedance of annular ring microstrip Antenna using circuit theory approach," IEEE Trans. Antennas & Propag., vol.AP-33, no.4, pp.369–374, April 1985.

[6] T. Fujimoto, K. Tanaka and M. Taguchi, "Wall admittance of circular microstrip antenna," IEICE Trans. Commun., vol.E82-B, no. 5, pp.760–767, May 1999.

[7] T. Fujimoto, K. Tanaka and M. Taguchi, "Analysis of elliptical microstrip antennas with and without a circular slot," IEICE Trans. Commun., vol.E83-B, no. 2, pp.386–393, Feb. 2000.

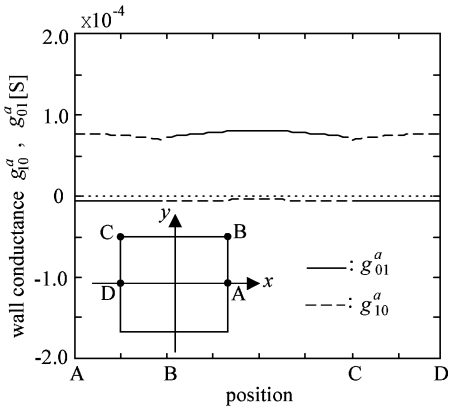

(a) Wall conductances

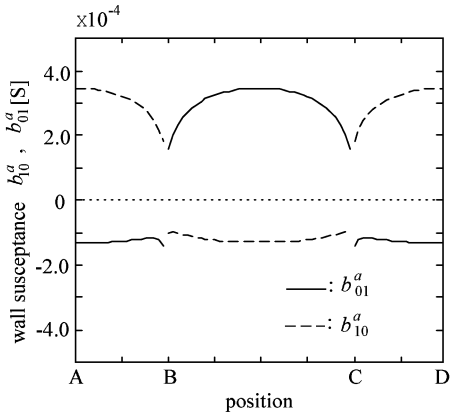

(b) Wall susceptances

Figure 6: Wall admittances of rectangular MSA with perturbation segments (W_1=7.46mm, L_1=7.30mm, W_0=3.73mm, L_0=3.65mm, h=0.764mm, ε_r=2.15, frequency=6.7GHz)

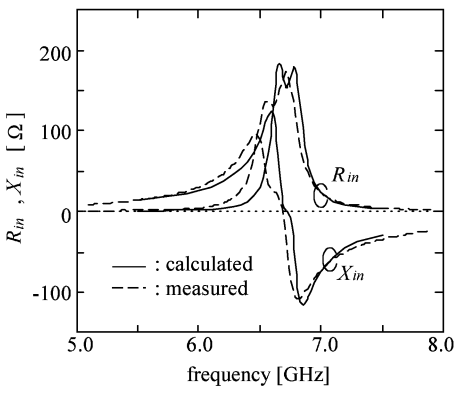

Figure 7: Input impedance of rectangular MSA with perturbation segments (W_1=7.46mm, L_1=7.30mm, W_0=3.73mm, L_0=3.65mm, h=0.764mm, ε_r=2.15, $\tan\delta$=0.001)